

## Magnetic susceptibility of YbN

Yu Zhou,\* S. P. Bowen, and D. D. Koelling  
*Argonne National Laboratory, Argonne, Illinois 60439*

R. Monnier

*Laboratorium für Festkörperphysik, ETH Hönggerberg, CH-8093 Zürich, Switzerland*

(Received 18 May 1990; revised manuscript received 4 September 1990)

Applying the Zwicknagl, Zevin, and Fulde (ZZF) approximation for the spectral densities of the occupied and empty  $f$  states resulting from a degenerate-Anderson-impurity model, which incorporates crystal fields, we compute the low-temperature magnetic susceptibility of YbN. The model, in which each crystal-field level couples to the band states with its own hybridization function, has previously been successfully applied without the ZZF approximation to explain the specific-heat structure at low temperatures. The ZZF approximation removes the spurious zero-temperature behavior of the parent noncrossing approximation for the susceptibility. Surprisingly, even at the low crystal-field degeneracy ( $N=2$ ) of YbN, the Shiba relation is very nearly satisfied. The appropriate experimental impurity susceptibility for comparison is extracted from the measurement by removing an empirical exchange interaction. The resultant Kondo temperature ( $T_0=8.49$  K) is consistent with previous specific-heat estimates (10–11 K), and the agreement with experiment is good.

### I. INTRODUCTION

Much effort has been expended on understanding the properties of hybridizing rare-earth systems such as the ytterbium monopnictides. The compact size of the Yb  $f$  orbitals severely limits the range of their interactions, and they are frequently approximated as an assembly of uncoupled impurities. Such rare-earth impurities in metals are commonly described by the infinite- $U$  degenerate Anderson mode.<sup>1</sup> For the severely restricted case in which the  $f$  orbital coupling to the band states is constant in energy and independent of orbital, the Bethe-ansatz formalism yields the exact ground-state and the thermodynamic properties<sup>2–5</sup> of the model. A numerical approach not suffering from these restrictions is the so-called noncrossing approximation NCA,<sup>6–10</sup> in which the magnetic degeneracy  $N$  is used as a self-consistent expansion parameter. Diagrammatic  $1/N$  expansion is performed to solve two coupled integral equations for the self-energy of empty and occupied  $f$  states, from which the spectral densities of these two  $f$  states can be derived. It is observed that the empty  $f$  spectral density  $\rho_0$  has a very sharp peak at an energy slightly below the  $f$  orbital energy<sup>7</sup> and a broad feature around the Fermi energy. The low-energy peak corresponds to the ground state of the interacting many particle system and, therefore, plays an important role in the low-temperature properties of the system. The broad features near the Fermi energy represent excited states of the system and should be less important at low temperatures. The specific heat of ytterbium pnictides in the presence of crystal fields (CF) with a doublet ground state has been calculated using NCA with reasonably satisfactory results.<sup>10</sup>

Experimentally, the magnetic susceptibility of these Yb pnictide materials changes from a Curie-like behavior at high temperature to a constant value, indicative of a nonmagnetic Fermi-liquid state, below a characteristic (Kondo) temperature.<sup>11,12</sup> Attempts to reproduce that behavior using the NCA for YbN, YbP, and YbAs (Ref. 10) have previously failed because the NCA does not satisfy certain Fermi-liquid relations (e.g., the Shiba relation) in the zero-temperature limit.<sup>7</sup> This non-Fermi-liquid behavior causes a singularity in the localized  $f$  moment spectral density at zero temperature, which leads to a divergent magnetic susceptibility at low temperatures.

Recently, Zwicknagl, Zevin, and Fulde<sup>13</sup> (ZZF) have proposed a scheme in which the low-energy peak in the empty  $f$  spectral function  $\rho_0$  is approximated as a  $\delta$  function, and other high-energy features of  $\rho_0$  are ignored. This approximation, to our benefit, does not exhibit the low-temperature spurious features of the NCA. Additionally, the magnitude of the numerical calculation for practical physical properties is significantly reduced. ZZF applied this scheme to a CF-split model in which the coupling between band states and impurity states was constant in energy. For this system, with an  $f$ -ground-state degeneracy of 6, the magnetic susceptibility at low temperature compares well with those obtained from the NCA. In this paper, we assess the ZZF approximation scheme for the susceptibility of YbN by calculating the low-temperature magnetic susceptibility in the presence of CF splittings where the lowest  $f$  level degeneracy is only 2, and we compare the results with recent experimental data.

### II. THE MODEL

In the presence of CF, the  $4f^{13} F_{7/12}$  multiplet of Yb is split into three levels:<sup>10</sup>  $\Gamma_6$  (ground state with energy  $\epsilon_6$ ,

degeneracy  $N_6=2$ ),  $\Gamma_8$  ( $N_8=4$ ) and  $\Gamma_7$  ( $N_7=2$ ). As described in detail in Refs. 14 and 10, we consider the infinite  $U$  limit of the degenerate Anderson model:

$$H^{U=\infty} = H_{\text{band}} + H_f^{U=\infty} + H_{\text{mix}}^{U=\infty} . \quad (1)$$

In the ZZF approximation, the spectral function  $\rho_0(\omega)$  of the empty  $4f$  state is

$$\rho_0(\omega) = (1 - n_f) \delta(\omega - \omega_0) , \quad (2)$$

where

$$\omega_0 = \varepsilon_6 - T_0 , \quad (3)$$

$n_f$  is the  $f$  valence at zero temperature, and  $T_0$  is the Kondo temperature. With Eq. (2), the spectral function  $\rho_i(\omega)$  of the occupied  $4f$  state can be obtained from an integral equation of the NCA:<sup>13,15</sup>

$$\rho_i(\omega) = \frac{1}{\pi} \frac{(1 - n_f) \gamma_i(\omega - \omega_0) f(\omega_0 - \omega)}{(\omega - \varepsilon_i)^2 + [(1 - n_f) \gamma_i(\omega - \omega_0) f(\omega_0 - \omega)]^2} , \quad (4)$$

where  $f(\omega)$  is the Fermi function

$$f(\omega) = \frac{1}{e^{\beta\omega} + 1} , \quad (5)$$

and  $\gamma_i(\omega) = \pi V^2(\omega)$  is the coupling width between band states and each CF level  $\Gamma_i$  as a function of energy deter-

mined using a tight-binding fit to an *ab initio* band-structure calculation.<sup>10</sup>

The relation between  $T_0$  and  $f$  valence  $n_f$  can be obtained for zero temperature using

$$n_f = \left[ \frac{1}{Z_f} \sum_i N_i \int_{-\infty}^{+\infty} d\omega e^{-\beta\omega} \rho_i(\omega) \right]_{T=0} , \quad (6)$$

where  $Z_f$  is the partition function of the  $4f$  electron

$$Z_f = (1 - n_f) e^{-\beta\omega_0} + \sum_i N_i \int_{-\infty}^{+\infty} d\omega e^{-\beta\omega} \rho_i(\omega) , \quad (7)$$

in which Eq. (2) has been used. With a spectral function given by Eq. (4), and setting the energy to zero at the Fermi energy, the relation between  $n_f$  and  $T_0$  follows the simple expression

$$n_f = \frac{C}{1 + C} , \quad (8)$$

where

$$C \equiv \frac{1}{\pi} \sum_i N_i \int_{-\infty}^0 \frac{\gamma_i(\omega)}{(\omega + \omega_0 - \varepsilon_i)^2} d\omega . \quad (9)$$

This same result can be derived from a variational approach.<sup>16,17</sup> Taking the hybridization width  $\gamma_i$  as a constant in energy, Eq. (8) can be further simplified to

$$n_f = (1 - n_f) \sum_i N_i \frac{\gamma_i}{\pi(T_0 + \varepsilon_i - \varepsilon_6)} , \quad (10)$$

which is exactly the same as Eq. (11a) in Ref. 13. However, with the energy-dependent  $\gamma_i(\omega)$  shown in Fig. 1(a) of Ref. 10, Eq. (9) is used throughout our calculations and discussions.

With CF levels  $\Gamma_6$  and  $\Gamma_8$ , the imaginary part of the dynamic susceptibility is<sup>7,13</sup>

$$\begin{aligned} \sigma_f(\omega, T) = & \frac{(1 - e^{-\beta\omega})}{3Z_f} \sum_i N_i \mu_i^2 \int_{-\infty}^{+\infty} d\varepsilon e^{-\beta\varepsilon} \rho_i(\varepsilon) \rho_i(\varepsilon + \omega) \\ & + \frac{(1 - e^{-\beta\omega})}{3Z_f} N_{68} \mu_{68}^2 \int_{-\infty}^{+\infty} d\varepsilon e^{-\beta\varepsilon} [\rho_6(\varepsilon) \rho_8(\varepsilon + \omega) + \rho_8(\varepsilon) \rho_6(\varepsilon + \omega)] , \end{aligned} \quad (11)$$

where  $\mu_i$  is the effective high-temperature moment for the level  $\Gamma_i$ . The appropriate theoretical magnetic moments for YbN are<sup>10</sup>

$$\mu_6 = \left[ \frac{16}{3} \right]^{1/2} \mu_B, \mu_8 = \left[ \frac{1040}{147} \right]^{1/2} \mu_B, \mu_7 = \left[ \frac{432}{49} \right]^{1/2} \mu_B , \quad (12a)$$

where  $\mu_B$  is the Bohr magneton. The van Vleck contribution is included in the second term of the summation in Eq. (11), in which

$$N_{68} \equiv (N_6 N_8)^{1/2} = (8)^{1/2} , \quad (12b)$$

$$\mu_{68} = g_{7/2}^2 \frac{70}{9} \frac{3}{N_{68}} \mu_B^2 ,$$

and  $g_{7/2}$  is the Lande factor (8/7).

The temperature dependence of the static susceptibility is given by:

$$\chi(T) = P \int_{-\infty}^{+\infty} d\varepsilon \frac{\sigma(\varepsilon, T)}{\varepsilon} . \quad (13)$$

### III. CALCULATIONS AND RESULTS

In the calculation, the integral in Eq. (11) was performed numerically using an FFT convolution algorithm. Consistent with the specific heat calculation,<sup>10</sup> the difference between the Fermi energy  $\varepsilon_F$  and the lowest CF level energy  $\varepsilon_6$  is taken as  $(\varepsilon_6 - \varepsilon_F) = -0.5$  eV. The value of the CF splitting  $(\varepsilon_8 - \varepsilon_6)$ , taken from a very recent inelastic neutron scattering study,<sup>18</sup> is 33 meV.<sup>19</sup> The  $\Gamma_7$  is considered sufficiently high that it is omitted from the calculation. While investigating the validity of ZZF approximation for various  $f$  orbital degeneracies,  $n_f$  is fixed at 0.94, and the Kondo temperature scale  $T_0$  is determined from Eq. (8). When comparing with experiment,  $T_0$  is treated as a free parameter to get the best fit

between the theory and experiment, and  $n_f$  is appropriately determined from Eq. (8).

To examine the validity of the ZZF approximation for the low-degeneracy ( $N_6 = 2$ ) YbN system, behavior of the dynamic susceptibility  $\sigma_f(\omega)$  for various lowest  $f$  level degeneracies ( $N_6 = 2, 3, 4, 5$ , and 6) is investigated (while the effects of any excited  $f$  state are ignored). The result shows that the spectral function of the lowest  $f$  levels  $\rho_6(\omega)$  has a well-defined single peak at energy  $\varepsilon_6$  as expected. Figure 1(a) is a plot of  $\sigma_f(\omega)/\omega$  at  $T \ll T_0$  for  $N_6 = 3, 4, 5$ , and 6. The case  $N_6 = 2$ , corresponding to YbN, is shown in Fig. 2(a). Despite the very different behavior for different  $N_6$ 's, it is seen that for no degeneracy does the dynamic susceptibility  $\sigma_f(\omega)/\omega$  diverge at  $\omega = 0$  in the low-temperature limit. This is a distinct advantage over the NCA,<sup>7</sup> in which  $\sigma_f(\omega)/\omega$  diverges as

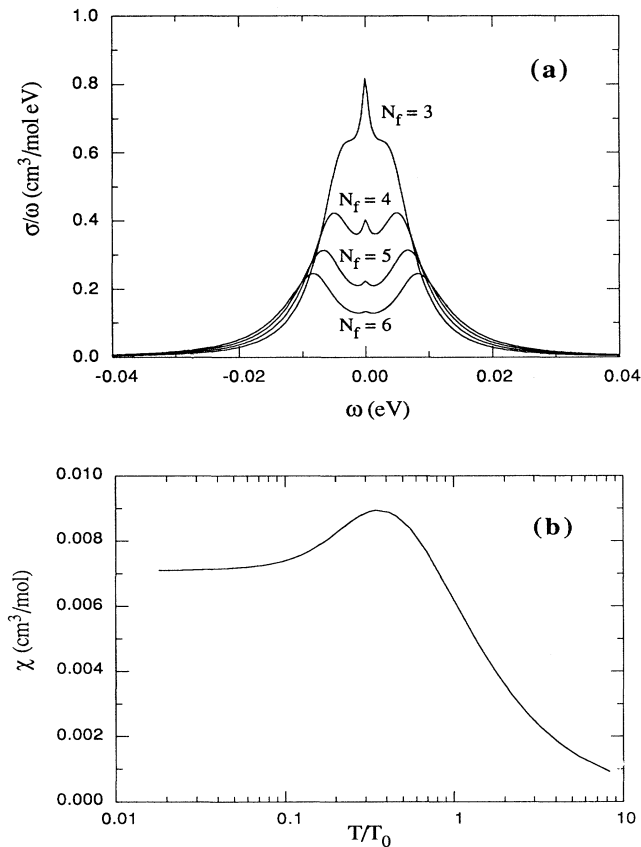


FIG. 1. Behavior of the imaginary part of the dynamical susceptibility divided by frequency  $[\sigma_f(\omega)/\omega]$  for different  $f$  degeneracies  $N_f$ , and static susceptibility  $\chi(T)$  for  $N_f = 6$ . The zero-temperature  $f$  occupancy  $n_f$  is set to 0.94 for all cases. (a) Low-temperature ( $T = 1.5$  K) behavior for  $\sigma_f(\omega)/\omega$  for  $N_f = 3, 4, 5$ , and 6, the corresponding Kondo temperature scales are  $T_0 = 40.8, 55.1, 69.5$ , and 84.1 K as determined from Eq. (8) in the text. Shiba relation is satisfied within a few percent for all four cases. (b) Susceptibility  $\chi(T)$  for  $N_f = 6$  with all parameters the same as in (a). Note that  $\chi(T)$  becomes a constant at low temperatures, and that a bump appears similar to the NCA results.

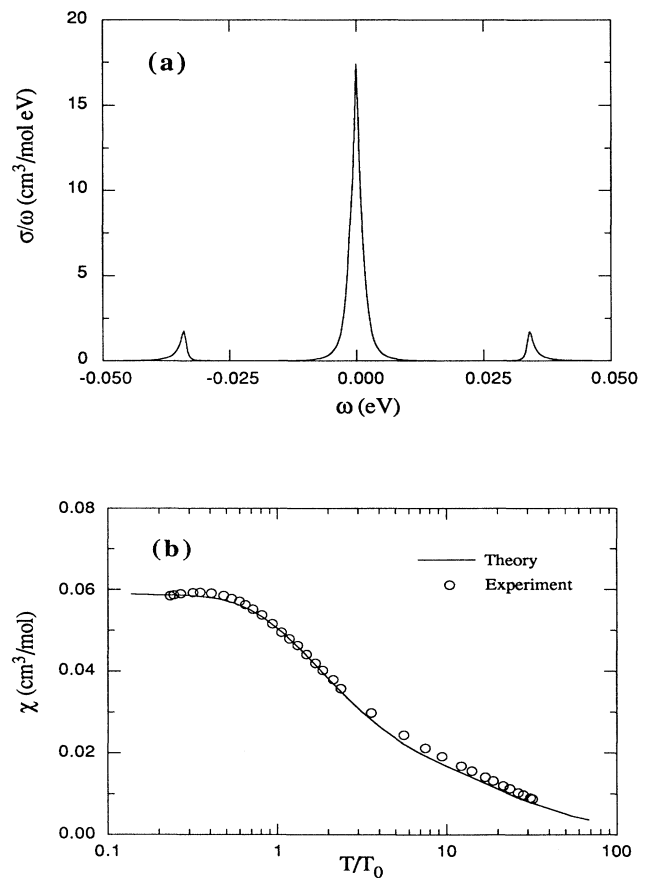


FIG. 2. Results of  $\sigma_f(\omega)/\omega$  and  $\chi(T)$  for YbN [ $T_0 = 8.49$  K adjusted for best fit with experimental result and  $n_f = 0.980$  determined from Eq. (8)]. (a) Low-temperature ( $T = 1.161$  K) behavior of  $\sigma_f(\omega)/\omega$  shows a peak at  $\omega = 0$  and two small features around  $\pm(\varepsilon_8 - \varepsilon_6)$ . (b) Both theoretical  $\chi(T)$  (solid line) and derived experimental  $\chi_f$  (circles) results are shown. Good agreement is obtained over the temperature range where the experiment was performed. However, theory does not reproduce the low temperature bump appearing in the experimental result.

$|\omega|^{-2/(N+1)}$ . The Fermi-liquid relation (Shiba relation)<sup>20</sup>

$$\frac{\sigma(\omega)}{\omega} \Big|_{\omega=0, T=0} = \frac{3\chi^2(T=0)}{N_6\mu_6^2} \quad (14)$$

is satisfied within a few percent for all values of  $N_6$ .

Figure 1(b) is the plot of  $\chi(T)$  as a function of temperature for  $N_6=6$ . For all values of  $N_6$  being studied the ZZF approximation gives a constant static susceptibility (Pauli law) at temperatures lower than  $T_0$ , indicating a nonmagnetic Fermi-liquid state, and has a finite limit as the temperature approaches zero.

To compare this contribution to the susceptibility with experimental data,<sup>21</sup> we subtracted the molecular field contribution from the experimental result using<sup>21-23</sup>

$$\frac{1}{\chi_m} = \frac{1}{\chi_f} - \lambda, \quad (15)$$

where  $\chi_m$  is the measured susceptibility,  $\chi_f$  is the experimentally derived contribution from the strongly interacting electrons in  $f$  orbitals, and  $\lambda$  is a molecular field constant in the exchange field  $H_E = \lambda M$ .  $\lambda$  is derived by extrapolating the high temperature  $1/\chi_m$  to  $T=0$ . From the experimental data of Ref. 21, we obtained  $\lambda = -10.9$  mol/cm<sup>3</sup>, with effective moment  $\mu_{\text{eff}} = 4.85\mu_B$  and Curie temperature  $T_C = -96.7$  K.

$\sigma_f(\omega)/\omega$  versus  $\omega$  for  $T \ll T_0$  and  $\chi(T)$  versus  $T$  are shown for YbN in Fig. 2. Due to the existence of CF splittings, it is seen in Fig. 2(a) that, in addition to the low-frequency feature of  $\sigma_f(\omega)/\omega$ , there are two peaks near  $\pm(\varepsilon_8 - \varepsilon_6)$ , arising from the van Vleck contributions to the susceptibility.  $T_0 = 8.49$  K is chosen to obtain the optimal fit with the  $\chi_f$  extracted from the experimental data using Eq. (15). This value of  $T_0$  is smaller than the value (10–11 K) obtained from the specific heat calculation with NCA. For comparison,  $\chi_f$  is also shown in Fig. 2(b). It is seen that reasonably good agreement is obtained at temperature range where experiment was performed. The bump observed at low-temperature cannot be reproduced in the calculation. If an alternative CF splitting  $(\varepsilon_8 - \varepsilon_6) = 55$  meV is used as in Ref. 10, the van

Vleck contribution to the susceptibility evaluation with Eq. (13) and the second term in Eq. (11) is much smaller, and the derived experimental impurity susceptibility is too large for the theory.

The agreement of the theory with experiment at low temperature shows that the ZZF approach has removed most of the difficulty encountered in the NCA calculation.<sup>10</sup> It is a little surprising that the Shiba relation is satisfied for this system with degeneracy as low as 2 since the approximation was derived from the NCA, which is only valid for large degeneracies. Even though the zero-temperature analytic solutions of the NCA offer some insights of why the Fermi-liquid relations are violated,<sup>24,25</sup> it is still not clear to us why the Shiba relation is satisfied within ZZF approximation regardless of  $f$  degeneracy.

#### IV. CONCLUSIONS

We have presented a calculation for the magnetic susceptibility of YbN in the presence of crystal fields. Using the ZZF approximation for the spectral function of the empty  $f$  state, the NCA low-temperature divergence of  $\sigma_f(\omega)/\omega$  at  $\omega=0$  is removed and the calculational effort greatly reduced. It is found that within this approximation the Fermi liquid relation for the dynamic susceptibility (Shiba relation) is satisfied within a few percent, even for a system with  $f$  degeneracy as low as 2, and a constant magnetic susceptibility at temperatures below Kondo temperature is obtained. The ZZF approximation sidesteps the deficiencies of the NCA and seems to yield good agreement with experiment even for small degeneracies. Using coupling functions  $V(\omega)$  determined from a tight-binding fit to a band structure calculation, the theoretical magnetic susceptibility of YbN clearly exhibits a nonmagnetic Fermi-liquid state in good agreement with experiment. The full explanation of its success has not yet been found.

#### ACKNOWLEDGMENTS

This work is supported by the U.S. Department of Energy, Basic Energy Sciences-Materials Sciences, under Contract No. W-31-109-ENG-38.

\*Permanent address: Department of Physics, Virginia Polytechnic Institute and State University, Blacksburg, Virginia 24061.

<sup>1</sup>P. W. Anderson, Phys. Rev. **124**, 41 (1961).

<sup>2</sup>A. M. Tsvelick and P. B. Wiegmann, J. Phys. C **15**, 1707 (1982); Adv. Phys. **32**, 453 (1983).

<sup>3</sup>N. Andrei, K. Furuya, and J. H. Lowenstein, Rev. Mod. Phys. **55**, 331 (1983).

<sup>4</sup>A. C. Hewson and J. W. Rasul, J. Phys. C **16**, 6799 (1985).

<sup>5</sup>J. W. Rasul and P. Schlottmann, Phys. Rev. B **39**, 3065 (1989).

<sup>6</sup>N. E. Bickers, D. L. Cox, and J. W. Wilkins, Phys. Rev. Lett. **54**, 230 (1985).

<sup>7</sup>N. E. Bickers, D. L. Cox, and J. W. Wilkins, Phys. Rev. B **36**, 2036 (1987).

<sup>8</sup>F. C. Zhang and T. K. Lee, Phys. Rev. B **30**, 1556 (1984).

<sup>9</sup>P. Coleman, Phys. Rev. B **29**, 3035 (1984).

<sup>10</sup>R. Monnier, L. Degiorgi, and B. Delley, Phys. Rev. B **41**, 573 (1990).

<sup>11</sup>See Ref. 1 of N. E. Bickers, D. L. Cox, and J. W. Wilkins, Phys. Rev. B **36**, 2036 (1987).

<sup>12</sup>A. Oyamada, S. Takagi, T. Kasuya, K. Sugiyama, and M. Date, J. Phys. Soc. Jpn. **57**, 3557 (1988).

<sup>13</sup>G. Zwirnagl, V. Zevin, and P. Fulde, Z. Phys. B **79**, 365 (1990).

<sup>14</sup>R. Monnier, L. Degiorgi, and D. D. Koelling, Phys. Rev. Lett. **56**, 2744 (1986).

<sup>15</sup>V. Zevin, G. Zwirnagl, and P. Fulde, Phys. Rev. Lett. **60**, 2331 (1988).

- <sup>16</sup>Q. Gunnarsson and K. Schönhammer, *Phys. Rev. B* **28**, 4315 (1983).
- <sup>17</sup>David C. Langreth, *Phys. Rev.* **150**, 516 (1966).
- <sup>18</sup>A. Dönni (unpublished).
- <sup>19</sup>The excitation energy of 55 meV attributed to the  $\Gamma_6$ - $\Gamma_8$  transition in Ref. 10 was shown in Ref. 18 to correspond to an optical phonon. The conclusions of Ref. 10 are not affected by this change in CF splitting.
- <sup>20</sup>H. Shiba, *Prog. Theor. Phys.* **54**, 967 (1975).
- <sup>21</sup>L. Degiorgi, W. Bacsa, and P. Wachter *Phys. Rev. B* **42**, 530 (1990).
- <sup>22</sup>A. Popielewicz, *Phys. Status Solidi B* **74**, 383 (1976).
- <sup>23</sup>R. J. Wojciechowski and L. Kowalewski, *Physica B* **153**, 24 (1988).
- <sup>24</sup>E. Müller-Hartmann, *Z. Phys. B* **57**, 281 (1984).
- <sup>25</sup>Y. Kuramoto and E. Müller-Hartmann, *J. Magn. Magn. Mater.* **52**, 122 (1985).